

CYCLIC DEFORMATION, CRACK GROWTH AND OXIDATION DAMAGE FOR NICKEL-BASED SUPERALLOYS

ZHAO Liguo

Loughborough University, Wolfson School of Mechanical and Manufacturing Engineering, Loughborough, United Kingdom, EU; L.Zhao@Lboro.ac.uk

Abstract

Viscoplasticity and crystal plasticity have been used to model cyclic deformation of nickel-based superalloys at elevated temperature. Model parameters were determined from strain-controlled cyclic test data, with consideration of strain rate effects. Model simulations are in good agreement with the experimental results for stress-strain loops, cyclic hardening behaviour and stress relaxation behaviour during the hold periods at the maximum and minimum strain levels. The models were also applied to study crack-tip deformation under fatigue, which showed the accumulation of permanent deformation at the crack tip due to plasticity-induced strain ratcheting. The strain accumulation was subsequently utilized as a criterion to predict crack propagation in a standard specimen using the finite element method, in comparison with experimental results. In addition, finite element analyses of oxygen penetration along grain boundaries have been carried out to quantify the fatigue-oxidation damage and calibrate the diffusion parameters based on FIB measurements of internal oxidation. A sequentially coupled mechanical-diffusion analysis was adopted to account for the effects of deformation on diffusion during fatigue loading. Prediction of oxidation-assisted crack growth has been carried out from finite element analyses of viscoplastic deformation and oxygen diffusion near a fatigue crack tip. The predictions compared well with the experimental results for triangular and dwell loading waveforms, with significant improvement achieved over those predicted from the mechanical model alone.

Keywords: Nickel superalloys, cyclic deformation, crack propagation, oxidation damage, computational modelling

1. INTRODUCTION

Nickel-based superalloys are favoured for disc rotors in high pressure compressor and turbine of aero-engines due to their exceptional mechanical properties at high temperature. Damage by low cycle fatigue, creep and oxidation is a major concern for disc rotors exposed to arduous gas environment for prolonged periods. Fatigue, creep and material constitutive behaviour of nickel alloys at high temperatures have been extensively studied in literature, both experimentally and numerically, to gain a fundamental understanding of time-dependent deformation behaviour of the materials [1, 2]. Evidence of oxidation in nickel alloys has also been presented for both smooth and cracked specimens with appreciable oxide layers built on free surfaces and at internal grain boundaries [3, 4]. Oxidation results in reduced fatigue life by promoting early cracking of surface oxide scales, followed by the dominantly intergranular cracking at accelerated growth rates [5, 6].

This work aims to achieve a mechanistic understanding of crack growth under fatigue-oxidation conditions by studying the relationship between deformation, oxidation damage and crack growth. The first objective of this work is to study the fundamental deformation behaviour of a nickel alloy, using the viscoplasticity and crystal plasticity constitutive models. With the assistance of these two models, detailed finite element analyses were carried out to study the stress-strain fields near a crack tip, which is the second objective of this work. Following this, the third objective is to model oxygen diffusion along grain boundaries and its effect on crack growth. Finally, crack growth rates were predicted under fatigue-oxidation conditions, with a comparison against the experimental results.

2. VISCOPLASTICITY AND CRYSTAL PLASTICITY MODELS

2.1. Viscoplasticity

The global material behaviour is described by the unified constitutive equations developed by Chaboche [7], where both isotropic (R) and kinematic hardening (α) variables are considered during the transient and saturated stages of cyclic response. A power-law relationship is adopted for the viscopotential and the viscoplastic strain rate $\dot{\epsilon}_p$ is expressed as [7]:

$$\dot{\epsilon}_p = \left\langle \frac{f}{Z} \right\rangle^n \frac{\partial f}{\partial \sigma} \text{ and } f(\sigma, \alpha, R, k_0) = J(\sigma - \alpha) - R - k_0 \leq 0, \quad (1)$$

where f is the von Mises yield function, Z and n are material constants, k_0 is the initial value of the radius of the yield surface and J denotes the von Mises distance in the deviatoric stress space, the brackets imply that $\langle x \rangle = x$ for $x > 0$ and $\langle x \rangle = 0$ for $x \leq 0$.

2.2. Crystal Plasticity

The material deformation at grain level was described by the crystal plasticity theory, where the flow rule is expressed in terms of slip resistance (S^α) and back stress (B^α) [8],

$$\dot{\gamma}_\alpha = \dot{\gamma}_0 \exp \left[\frac{-F_0}{k\theta} \left\langle 1 - \left\langle \frac{|\tau^\alpha - B^\alpha| - S^\alpha \mu / \mu_0}{\hat{\tau}_0 \mu / \mu_0} \right\rangle^{p_0} \right\rangle^{q_0} \right] \text{sgn}(\tau^\alpha - B^\alpha), \quad (2)$$

where k is the Boltzmann constant, τ^α is the resolved shear stress on the slip system α , θ the absolute temperature, μ and μ_0 the shear moduli at θ and 0 Kelvin, respectively, and F_0 , $\hat{\tau}_0$, p_0 , q_0 and $\dot{\gamma}_0$ are material constants. The two internal variables, the slip resistance in each slip system, S^α , and the back stress, B^α , are introduced at the slip system level, which represent the state associated with the current dislocation network.

2.3. Model Parameters and UMAT

Both the viscoplasticity and crystal plasticity formulation were implemented numerically into the finite element (FE) code ABAQUS via a user-defined material subroutine (UMAT), where the fully implicit (Euler backward) integration algorithm was adopted. For crystal plasticity, a three-dimensional representative volume element, consisting of randomly oriented grains, was built for the finite element analyses under periodic boundary constraints. Values of the model parameters were optimized from the uniaxial experimental data of a nickel alloy RR1000 at 650°C, by fitting the measured viscoplastic material response for a range of strain-controlled loading conditions [1].

3. MODELLING OF STRESS-ASSISTED OXYGEN DIFFUSION

Here we are concerned with the stress-assisted diffusive transport of oxygen into the material, which can be modelled as [9]:

$$\frac{\partial C}{\partial t} = \nabla(D\nabla C - DCM\nabla P), \quad (3)$$

where C is the concentration of oxygen, t the time, ∇ the gradient, D the oxygen diffusivity, P the hydrostatic stress (pressure) and M the pressure factor. The gradient of hydrostatic stress (or pressure) is regarded as the driving force for stress-assisted diffusion process.

4. FE MODEL AND PROCEDURE

A standard compact tension specimen was considered for crack tip deformation analyses. The finite element mesh for the whole specimen consists of four-node, first-order elements with full integration. For pure fatigue loading, a triangular waveform was used and frequencies varied from 0.001 Hz to 2.5 Hz. For dwell loading, a trapezoidal waveform was used with a 1-x-1-1 pattern, where x is the dwell time and varies from 1 s to 1000 s [2]. The crack length was chosen to be half of the specimen width. FE submodelling was adopted to study the dependence of crack tip deformation on the grain microstructure. The submodel was constructed near the crack tip and contains 150 grains with randomly assigned orientations, where the loading was prescribed by the displacements of its boundaries obtained from the global model analyses. The same model was also used for oxygen diffusion analyses along grain boundaries, for which grain boundaries were meshed into one-dimensional diffusion elements, sharing the same nodes with the grain interior elements.

5. RESULTS AND DISCUSSIONS

5.1. Modelling of Cyclic Deformation

The simulated stress-strain responses for monotonic and the first cycle of fatigue loading are shown in **Fig. 1** for the strain rate of 0.05 %/s, with a direct comparison against the experimental data [1]. Clearly, the model simulations agree very well with the test data. The stress response and the shape of hysteresis loops were both well captured by the both viscoplasticity and crystal plasticity models, as well as the simulated stress relaxation during the strain hold periods.

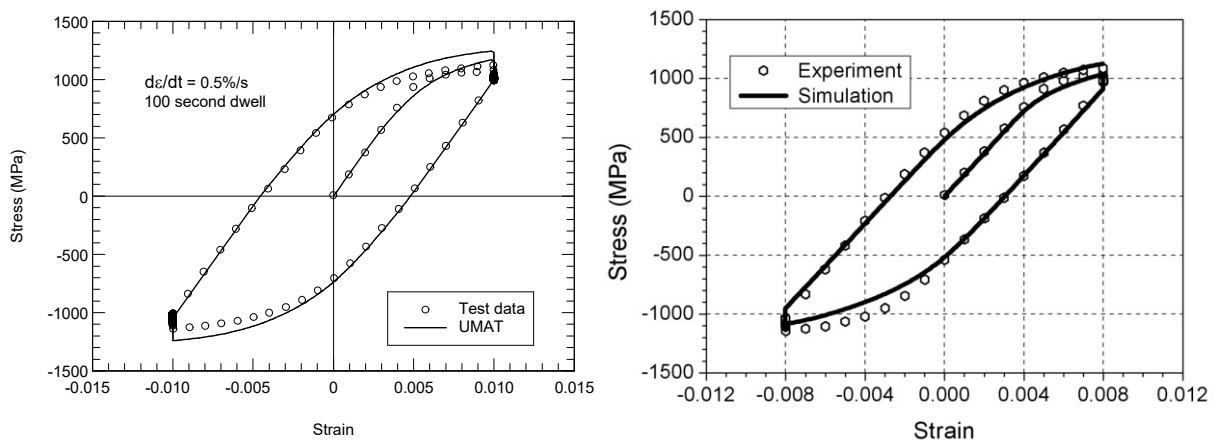


Fig. 1 Comparison of simulations and experimental data for the first cycle of a strain-controlled cyclic test with a superimposed 100-second dwell period at both maximum and minimum loads: viscoplasticity (left) and crystal plasticity (right)

5.2. Modelling of Crack-Tip Deformation

Contour plot of the von Mises stress near the crack tip confirms the well-known butterfly shape for viscoplasticity simulation. However, for crystal plasticity simulation, grain microstructure is shown to have an influence on the Mises stress contour zone which does not have the butterfly shape. The stress concentration zone obtained from the crystal plasticity analyses seems to be of an arbitrary shape and is less severe than that obtained from the visco-plasticity analyses, indicating the significant effect of grain microstructure on crack tip stress field (**Fig. 2**).

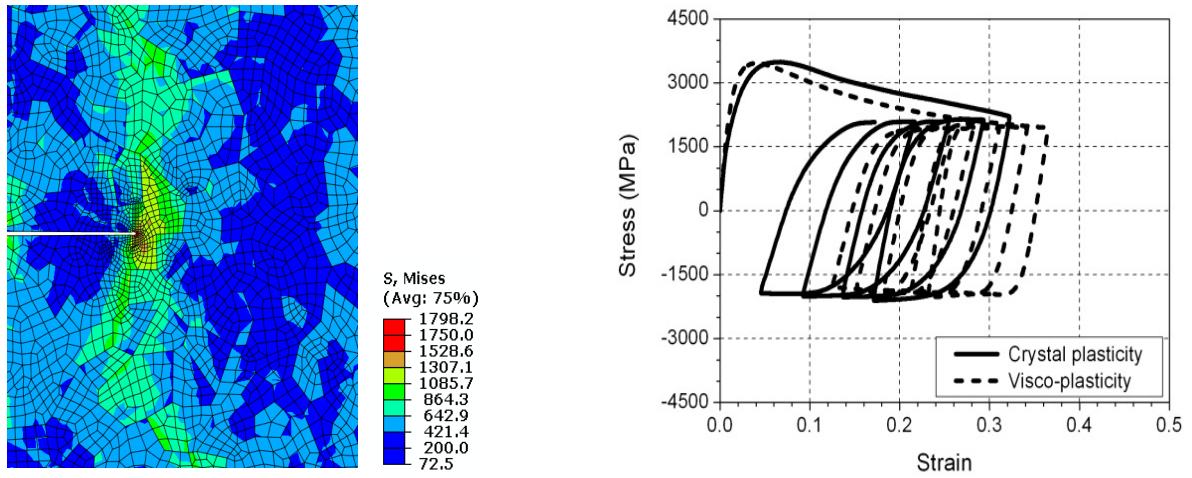


Fig. 2 Contour plots of the von Mises stress obtained from the crystal plasticity model (left) and comparison of the stress-strain response ahead of the crack tip for crystal plasticity and viscoplasticity models (right)

The stress-strain response normal to the crack, averaged over a distance of $0.40\ \mu\text{m}$ ahead of the crack tip, is shown in **Fig. 2**, in a comparison with those obtained from the continuum viscoplasticity analyses. For both cases, the cyclic stress-strain loops remain open and exhibit a so-called ratchetting phenomenon, where the plastic deformation during the loading portion is not balanced by an equal amount of yielding in the reverse loading direction. This leads to strain accumulation near the crack tip with the number of fatigue cycles.

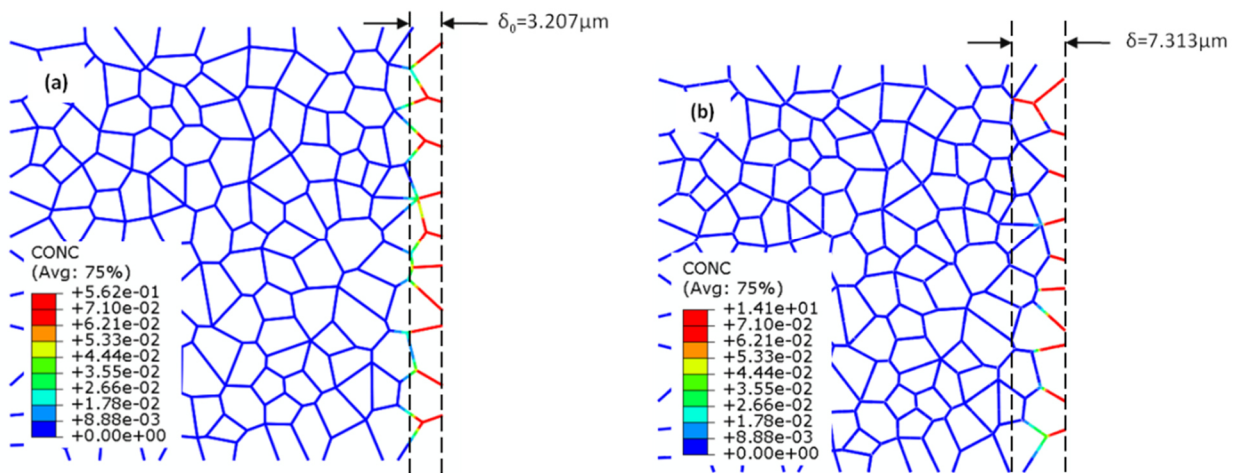


Fig. 3 Simulated oxygen concentration at 800°C for natural diffusion (left) and fatigue-assisted diffusion (right)

5.3. Modelling of Oxygen Diffusion

Modelling of oxygen diffusion confirmed that fatigue loading tends to induce a non-uniform distribution of oxygen concentration (**Fig. 3b**) along the grain boundaries when compared to the case for natural diffusion (**Fig. 3a**), with increased depth of oxygen penetration into the grain boundaries. This is also supported by the FIB measurements of internal oxidation damage which occurs mainly along the grain boundaries and becomes more severe with the increase of stress level [4].

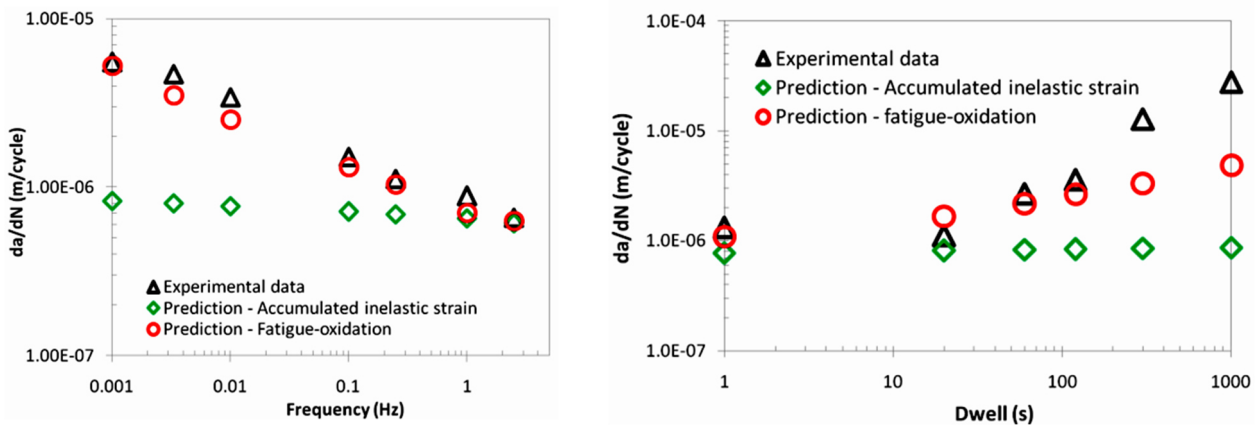


Fig. 4 The effects of loading frequency (left) and dwell times (right) on crack growth rates. Comparison of model predictions against experimental results [2]

5.4 Prediction of crack growth under fatigue-oxidation conditions

Here, two parameters, namely the accumulated inelastic strain and oxygen concentration, were used to represent the contributions of viscoplastic deformation and oxidation damage to crack growth. The critical values of the two parameters were back calculated from experimental crack growth data for arrange of loading frequencies at $\Delta K = 30 \text{ MPa}\sqrt{\text{m}}$ [2]. Using the two parameters, the predicted effects of loading frequency on crack growth rates is shown in **Fig. 4a** for $\Delta K = 40 \text{ MPa}\sqrt{\text{m}}$, in comparison with the test data for CT specimens at $650 \text{ }^\circ\text{C}$ [2]. For the predictions based on fatigue-oxidation failure curve, an excellent agreement was achieved for all loading frequencies. The predicted effects of dwell time on crack growth rates is shown in **Fig. 4b** for $\Delta K = 40 \text{ MPa}\sqrt{\text{m}}$, in a direct comparison with test data for CT specimens at 650°C [2]. The predictions from accumulated inelastic strain show increased deviation from the experimental data as the dwell period is increased, especially when a dwell period is over 60 seconds. Again, this difference is much reduced when the fatigue-oxidation failure criterion was used for the prediction.

6. CONCLUSIONS

Viscoplasticity and crystal plasticity modelling of cyclic deformation has been presented for a polycrystalline nickel-based superalloy at elevated temperature. The models were also applied to study the near-tip deformation for a crack in a CT specimen, showing distinctive strain accumulation behaviour near the crack tip. Oxygen diffusion analyses have been carried out to quantify oxidation damage and associated crack growth. A two-parameter failure criterion, based on accumulated inelastic strain and oxygen concentration near the crack tip, was successful to predict crack growth rates under fatigue-oxidation conditions.

ACKNOWLEDGEMENTS

The work was funded by the EPSRC (Grant EP/E062180/1) of the UK. LGZ acknowledges the support from the Royal Society and the Leverhulme Trust of the UK for a Senior Research Fellowship (10/2008~09/2009).

REFERENCES

- [1] ZHAN Z.L., TONG J. A study of cyclic plasticity and viscoplasticity in a new nickel-based superalloy using unified constitutive equations, Part I: Evaluation and determination of material parameters. *Mechanics of Materials*, Vol. 39, 2007, pp. 64-72.
- [2] DALBY S., TONG J. Crack growth in a new nickel-based superalloy at elevated temperature, Part I: Effects of loading waveform and frequency on crack growth. *Journal of Materials Science*, Vol. 40, 2005, pp. 1217-1228.

- [3] BERGER P., MOULIN G., VIENNOT M. Nuclear microprobe study of stress-oxidation of nickel. Nuclear instruments and methods in physics research. Section B: Beam interactions with materials and atoms, Vol. 130, 1997, pp. 717-721.
- [4] KARABELA A., ZHAO L.G., TONG J., SIMMS N.J., NICHOLLS J.R., HARDY M.C. Effect of cyclic stress and exposure temperature on oxidation damage for a nickel-based superalloy. Materials Science and Engineering A, Vol. 528, 2011, pp. 6194-6202.
- [5] PFAENDTNER J.A., MCMAHON Jr. C.J. Oxygen-induced intergranular cracking of a Ni-base alloy at elevated temperatures – an example of dynamic embrittlement. Acta Materialia, Vol. 49, 2001, pp. 3369-3377.
- [6] KRUPP U., KANE W.M., LAIRD C., MCMAHON Jr. C.J. Brittle intergranular fracture of a Ni-base superalloy at high temperatures by dynamic embrittlement. Materials Science and Engineering A, Vol. 387-389, 2004, pp. 409-413.
- [7] CHABOCHE J.L. Constitutive equations for cyclic plasticity and cyclic viscoplasticity. International Journal of Plasticity, Vol. 5, 1989, pp. 247-302.
- [8] BUSSO E.P. Cyclic Deformation of monocrystalline nickel aluminide and high temperature coatings. PhD thesis, Massachusetts Institute of Technology, Cambridge, MA, USA, 1990.
- [9] CARRANZA F.L., HABER R.B. A Numerical study of intergranular fracture and oxygen embrittlement in an elastic-viscoplastic solid. Journal of the Mechanics and Physics of Solids, Vol. 47, 1999, pp. 27-58.